G3: Genes|Genomes|Genetics Early Online, published on September 10, 2019 as doi:10.1534/g3.119.400704

Pharmaco-Genetic Screen To Uncover Actin Regulators Targeted by Prostaglandins During *Drosophila* Oogenesis

Andrew J. Spracklen[a], Maureen C. Lamb, Christopher M. Groen[b], and Tina L. Tootle*
*corresponding author

Anatomy and Cell Biology, Carver College of Medicine; University of Iowa, Iowa City, IA 52242, USA

[a]Present address: Department of Biology, University of Massachusetts, Amherst, MA, 01003

[b]Present address: Regenerative Neurobiology Laboratory, Mayo Clinic, Rochester, MN 55905

Running Title: Screen for prostaglandin targets

Keywords: *Drosophila melanogaster*, prostaglandins, Enabled, Capping Protein, Non-muscle myosin II regulatory light chain

Corresponding author: Tina L. Tootle, University of Iowa, 51 Newton Rd, 1-550BSB, Iowa City, IA, 52242. Phone: (319)335-7763. Email: tina-tootle@uiowa.edu

ABSTRACT

Prostaglandins (PGs) are lipid signaling molecules with numerous physiologic functions, including pain/inflammation, fertility, and cancer. PGs are produced downstream of cyclooxygenase (COX) enzymes, the targets of non-steroidal anti-inflammatory drugs (NSAIDs). In numerous systems, PGs regulate actin cytoskeletal remodeling, however, their mechanisms of action remain largely unknown. To address this deficiency, we undertook a pharmaco-genetic interaction screen during late-stage *Drosophila* oogenesis. *Drosophila* oogenesis is as an established model for studying both actin dynamics and PGs. Indeed, during Stage 10B, cage-like arrays of actin bundles surround each nurse cell nucleus, and during Stage 11, the cortical actin contracts, squeezing the cytoplasmic contents into the oocyte. Both of these cytoskeletal properties are required for follicle development and fertility, and are regulated by PGs. Here we describe a pharmaco-genetic interaction screen that takes advantage of the fact that Stage 10B follicles will mature in culture and COX inhibitors, such as aspirin, block this *in vitro* follicle maturation. In the screen, aspirin was used at a concentration that blocks 50% of the wild-type follicles from maturing in culture. By combining this aspirin treatment with heterozygosity for mutations in actin regulators, we quantitatively identified enhancers and suppressors of COX inhibition. Here we present the screen results and initial follow-up studies on three strong enhancers – Enabled, Capping protein, and non-muscle Myosin II Regulatory Light Chain. Overall, these studies provide new insight into how PGs regulate both actin bundle formation and cellular contraction, properties that are not only essential for development, but are misregulated in disease.

INTRODUCTION

Many physiological functions, including pain/inflammation, reproduction, heart health/disease, and cancer, are mediated by lipid signals termed prostaglandins (PGs) (TOOTLE 2013). PGs are produced at their site of action by cyclooxygenase (COX) enzymes, which are inhibited by non-steroidal anti-inflammatory drugs (NSAIDs). One cellular target of PGs is the actin cytoskeleton (HALBRUGGE *et al.* 1990; NOLTE *et al.* 1991; KAWADA *et al.* 1992; PEPPELENBOSCH *et al.* 1993; ASZODI *et al.* 1999; PIERCE *et al.* 1999; BANAN *et al.* 2000; BEARER *et al.* 2002; DORMOND *et al.* 2002; MARTINEAU *et al.* 2004; BULIN *et al.* 2005; BIRUKOVA *et al.* 2007). However, the mechanisms by which PGs regulate actin remodeling remain largely unknown. To address this, we undertook a screen to identify the specific targets of PGs during *Drosophila* oogenesis.

Drosophila oogenesis provides a powerful model for uncovering the mechanisms by which PGs regulate actin remodeling (SPRACKLEN AND TOOTLE 2015). Actin-dependent morphogenic events necessary for mid-to-late stage follicle development (Figure 2A) are regulated by the coordinated activity of numerous actin binding proteins [reviewed in (HUDSON AND COOLEY 2002)]. There are 14 stages of follicle development. Each follicle consists of 16 germline-derived cells – an oocyte and 15 support cells, termed nurse cells – and ~1,000 somatically-derived follicle cells. During Stage 10B (S10B), cage-like arrays of parallel actin filament bundles rapidly extend from the nurse cell membranes toward the nuclei (GUILD *et al.* 1997; HUELSMANN *et al.* 2013). These bundles hold the nuclei in place during Stage 11 (S11), when the nurse cells undergo a rapid actomyosin-based contraction to transfer their cytoplasmic contents into the expanding oocyte in a process termed nurse cell dumping (WHEATLEY *et al.* 1995). Nurse cell dumping requires PGs, as loss of the *Drosophila* COX-like enzyme Pxt blocks this process (TOOTLE AND SPRADLING 2008). Specifically, PGs are required for bundle formation, cortical actin integrity, and cellular contraction (Figure 1C-D compared to Figure 1A-B; (TOOTLE AND SPRADLING 2008; GROEN *et al.* 2012).

Multiple lines of evidence indicate PGs directly regulate actin remodeling. First, mRNA levels of actin regulators are unchanged in *pxt* mutants (TOOTLE *et al.* 2011). This has been verified at the protein level for a number of actin binding proteins (GROEN *et al.* 2012; SPRACKLEN *et al.* 2014). Second, pharmacologic disruption of PG signaling acutely disrupts actin remodeling (TOOTLE AND SPRADLING 2008), suggesting that PGs likely post-translationally regulate actin binding proteins to rapidly modulate actin remodeling. Together these data led us to hypothesize that PG signaling coordinates the activities of multiple actin regulators to promote both actin remodeling during S10B and cellular contraction during S11.

Here we present the results of a pharmaco-genetic interaction screen to identify actin binding proteins functioning downstream of PG signaling during S10B-11 of *Drosophila* oogenesis. This screen tested factors previously implicated in regulating nurse cell dumping and/or follicle morphogenesis during mid-oogenesis. We identified a number of actin regulators and interacting proteins including Capping protein (Cp; *Drosophila* Cpa and Cpb), E-Cadherin (*Drosophila* Shotgun, Shg), Enabled (Ena), Fascin (*Drosophila* Singed, Sn), Lamellipodin (*Drosophila* Pico), and the non-muscle Myosin II Regulatory Light Chain (MRLC; *Drosophila* Spaghetti squash, Sqh) as candidate downstream targets of PG signaling. Here, we present a summary of the screen results and follow-up studies on Ena, Cp, and MRLC.

MATERIALS AND METHODS

Fly husbandry

Fly stocks were maintained at 21°C on standard cornmeal-agar-yeast food. Flies were fed with wet yeast paste daily and aged for 3-5 days for *in vitro* follicle maturation (IVEM) assays and ovary analyses, including immunofluorescence and immunoblotting. y^1w^1 (*yw*) was used as the wild-type control in experiments. Two *pxt* alleles were used: pxt^{f01000} (pxt^f) and $pxt^{EY03052}$ (pxt^{EY}). The sources of stocks used in the pharmaco-genetic interaction screen are indicated in Table S1.

In vitro follicle maturation (IVEM)

IVEM assays were performed as previously described (TOOTLE AND SPRADLING 2008; SPRACKLEN AND TOOTLE 2013). Briefly, for each genotype analyzed, whole ovaries were dissected out of mated adult females in room temperature IVEM media (10% heat inactivated fetal bovine serum (FBS) (Atlanta Biologicals, Flowery Branch, GA, USA), 1X penicillin/streptomycin (100X penicillin/streptomycin, Gibco, Life Technologies, Carlsbad, CA, USA), in Grace's insect media (Lonza, Walkersville, MD, USA)) into a 9-well glass plate using forceps. Ovaries were immediately transferred to a clean well with fresh IVEM media and Stage 10B (S10B) follicles were isolated using dissecting needles mounted in pin vises and transferred to a clean well. Once 20-30 S10B follicles per condition were isolated, they were transferred to a clean well in a 24-well plate (Figure 2B). Any IVEM media transferred with the follicles was gently aspirated using a pulled Pasteur pipette and immediately replaced with 1 mL of IVEM media containing vehicle only (3µl of 100% ethanol per 1 mL of IVEM media) or 1.5mM aspirin (3µl of 0.5M aspirin [Cayman Chemical, Ann Arbor, MI, USA] in 100% ethanol per 1 mL of IVEM media). Treated follicles were allowed to mature overnight at room temperature. The assay was scored by determining the percentage of follicles that completed nurse cell dumping in each condition. This was determined by assessing whether the follicles stalled at S10B or whether they progressed to Stage 11 (S11), 12 (S12), or 13/14 (S13/14) based on overall follicle morphology (Figure 2A). Follicles scored as S10B or S11 were considered to have not completed nurse cell dumping, while follicles that reached S12 or S13/14 were considered to have completed nurse cell dumping (Figure 2C-F, red * indicates follicles that failed to dump).

Screen analysis

In order to compare genotypes across the screen, we calculated a dumping index for each replicate (Figure 2H). The dumping index:

$$\frac{\%\ follicles\ dumping\ in\ aspirin\ media}{\%\ follicles\ dumping\ in\ control\ media}$$

Average dumping indices and standard deviations for each experimental genotype and their corresponding controls are reported in Table S1. To aid in the identification of potential interactions in this screen, we focused on differences in the dumping index between experimental genotypes and wild-type controls by normalizing the data. For a given experiment, the wild-type controls were set to zero, and the normalized experimental dumping index was calculated as: $Experimental\ dumping\ index - Control\ dumping\ index$ (Figure 2H). Figure 2I provides the data and calculations for two representative experiments. The average normalized dumping index, and their standard deviation, for all data are plotted in Figure 3. For the purpose of this screen, we arbitrarily defined strong interactors as those showing a response of greater than three standard deviations from wild-type controls, weak interactors as those showing a response between one and three standard deviations from wild-type controls, and non-interactors showing a response of less than one standard deviation from wild-type controls in their ability to modify sensitivity to COX inhibition. For statistical analyses, we used an ordinary one-way ANOVA and Dunnett's multiple comparisons test to compare means between experimental and control groups. Graphs generated and statistical comparisons made using Prism8 (GraphPad Software, La Jolla, CA, USA).

Western blots

Approximately 5 whole ovary pairs were dissected in room temperature Grace's insect media (Lonza, Walkersville, MD, USA or Thermo Fisher Scientific, Waltham, MA), transferred to a 1.5ml microcentrifuge tube containing 50µL of Grace's media, an equal volume of 2X SDS Sample Buffer was added and the tissue lysed by grinding with a plastic pestle. Western blots were performed using standard methods. The following primary antibodies were used: mouse α–Enabled (5G2) (Goodman, C.; obtained from the Developmental Studies Hybridoma Bank (DSHB), 1:200; rabbit α-Zipper (Karess, R.; Institut Jacques Monod, Paris, France; (WHEATLEY *et al.* 1995)), 1:1000; and mouse α–αTubulin T9026 (Sigma-Aldrich, St. Louis, MO, USA), 1:5000. All blots had 0.1% Tween 20 added to the primary antibody in 5% milk diluted in 1×

Tris-buffered saline. The following secondary antibodies were used: Peroxidase-AffiniPure Goat Anti-Mouse IgG (H+L), 1:5000 and Peroxidase-AffiniPure Goat Anti-Rabbit IgG (H+L), 1:5000 (Jackson ImmunoResearch Laboratories, West Grove, PA, USA). Blots were developed with SuperSignal West Pico or Femto Chemiluminescent Substrate (Thermo Scientific, Waltham, MA, USA) and imaged using the ChemiDoc-It Imaging System and VisionWorksLS software (UVP, Upland, CA, USA) or Amersham Imager 600 (GE Healthcare Life Sciences, Chicago, IL). Bands were quantified using densitometry analysis in ImageJ (ABRAMOFF *et al.* 2004). Ena levels were assessed using 2 independent biological samples, Zipper levels were assessed using 3 independent biological samples, and statistical significance was determined using a two-sample t-test with unequal variance in Excel (Microsoft, Redmond, WA, USA).

Immunofluorescence

Whole ovaries were dissected in room temperature Grace's insect media (Thermo Fisher Scientific, Waltham, MA). For phalloidin staining, samples were fixed for 10 minutes at room temperature in 4% paraformaldehyde in Grace's insect media. Briefly, samples were blocked using antibody wash (1X phosphate-buffered saline, 0.1% Triton X-100, and 0.1% bovine serum albumin) six times for 10 minutes each. Alexa Fluor 568-conjugated phalloidin (Thermo Fischer Scientific) used in at a concentration of 1:250 in both primary and secondary antibody solutions overnight. Six washes in antibody wash (10 min each) were performed after both the primary and secondary antibody incubations.

Active-MRLC staining was performed using a protocol provided by Jocelyn McDonald (MAJUMDER *et al.* 2012; ARANJUEZ *et al.* 2016). Briefly, ovaries were fixed for 20 min at room temperature in 4% paraformaldehyde in 1X phosphate-buffered saline (PBS) and 0.2% Triton X-100. Samples were blocked by incubating in Triton antibody wash (1XPBS, 0.2% Triton X-100, and 5% bovine serum albumin [BSA]) for 30 min. Primary antibodies were incubated for at least 30 hours at 4°C. The rabbit anti-pMRLC (S19; Cell Signaling, Davers, MA) was diluted 1:125 in Triton antibody wash. Alexa Fluor 647–phalloidin (Invitrogen, Life Technologies, Grand Island,

NY) was included with both primary and secondary antibodies at a concentration of 1:250. After six washes in Triton antibody wash (10 min each), the secondary antibody Alexa Fluor 488=-conjugated goat anti-rabbit (Invitrogen, Life Technologies) was diluted 1:500 in Triton antibody wash and incubated overnight at 4°C. Samples were washed six times in Triton antibody wash (10 min each).

After the final wash for all samples, 4',6-diamidino-2-phenylindole (DAPI, 5 mg/mL) staining was performed at a concentration of 1:5000 in 1XPBS for 10 min at room temperature. Ovaries were mounted in 1 mg/ml phenylenediamine in 50% glycerol, pH 9 (Platt and Michael, 1983). All experiments were performed a minimum of three independent times.

Image acquisition and processing

Confocal z-stacks of *Drosophila* follicles were obtained using LAS AS SPE Core software on a Leica TCS SPE mounted on a Leica DM2500 using an ACS APO 20x/0.60 IMM CORR -/D objective (Leica Microsystems, Buffalo Grove, IL) or Zen software on a Zeiss 700 LSM mounted on an Axio Observer.Z1 using a Plan-Apochromat 20x/0.8 working distance (WD) = 0.55 M27 (Carl Zeiss Microscopy, Thornwood, NY). Maximum projections (2-4 confocal slices), merged images, rotation, cropping, and pseudocoloring, including rainbow RGB intensity coloring, were performed using ImageJ software (ABRAMOFF *et al.* 2004).

p-MRLC intensity quantification

Quantification of p-MRLC was performed on maximum projections of 2 confocal slices of similar focal planes of a 20x confocal image using ImageJ software (ABRAMOFF *et al.* 2004). Briefly, the average fluorescent intensity was measured for the same length along one of the posterior nurse cell membranes. The average fluorescent intensity was also measured for the cytoplasm of the same nurse cell and subtracted from the membrane intensity to correct for variations in stain intensity. Raw data was compiled in Excel (Microsoft, Redmond, WA).

Graphs were generated and Student's t-test performed using Prism8 (GraphPad Software, La Jolla, CA, USA).

Data and reagent availability

Fly stocks and detailed protocols are available upon request. The authors affirm that all data necessary for confirming the conclusions of the article are present within the article, figures, and the supplementary table uploaded to figshare.

RESULTS AND DISCUSSION

Pharmaco-genetic interaction screen

To identify actin regulators and interacting proteins acting downstream of PG signaling during S10B of *Drosophila* oogenesis, a pharmaco-genetic interaction screen was undertaken. This screen took advantage of the following: 1) S10B follicles mature to S14 in *in vitro* culture conditions (Figure 2B-C; (TOOTLE AND SPRADLING 2008; SPRACKLEN AND TOOTLE 2013)), 2) COX inhibitor treatment suppresses follicle maturation (Figure 2D; (TOOTLE AND SPRADLING 2008; SPRACKLEN AND TOOTLE 2013), and 3) multiple mutant alleles of most actin regulators and interacting proteins are readily available. In this screen we focused on small set of actin regulators previously implicated in regulating nurse cell dumping and/or follicle morphogenesis during mid-oogenesis.

We hypothesized that if a particular actin regulator were a downstream target of PG signaling, then reduced levels of that actin regulator (i.e., through heterozygosity for strong alleles or homozygosity for weak alleles) would enhance or suppress the inhibition of nurse cell dumping and subsequent follicle maturation due to COX inhibitor treatment; reduced levels alone are not predicted to block nurse cell dumping. For example, if PG signaling positively regulates Protein X to promote actin remodeling during S10B, then heterozygosity for a strong allele of *protein x* would be expected to enhance follicle sensitivity to COX inhibition and result in less follicles completing dumping (Figure 2E, G, enhancement). However, if PG signaling

negatively regulates Protein Y to promote actin remodeling during S10B, then heterozygosity for a strong allele of *protein y* would be expected to suppress follicle sensitivity to COX inhibition and results in more follicles completing dumping (Figure 2F, G suppression). In contrast, reduced levels of an actin binding protein that is not a downstream target of PG signaling during S10B would not be expected to modify follicle sensitivity to COX inhibition (Figure 2G, non-interactor).

Based on this rationale, we conducted the first pass of a pharmaco-genetic interaction screen using a concentration of aspirin (1.5mM) empirically determined to reproducibly inhibit ~50% of a population of wild-type S10B follicles from completing nurse cell dumping in culture (Figure 2D; (TOOTLE AND SPRADLING 2008)). Using this dose of aspirin ensured we could readily observe both suppression and enhancement of follicle sensitivity to COX inhibition (Figure 2E-F). For each genotype tested, isolated S10B follicles (~20-30 follicles per condition) were cultured overnight in either vehicle-treated or aspirin-treated media and the percentage of follicles completing dumping was quantified. Follicles in S10B-11 were considered to have not completed dumping, while those in S12-14 were scored as completing nurse cell dumping (Figure 2A, C-F; red * indicates follicles that failed to dump). To normalize the data for any genotypic variation related to *in vitro* follicle maturation, we calculated the ratio of the percentage of follicles completing nurse cell dumping in aspirin-treated media to the percentage of follicles completing nurse cell dumping in control media for each genotype analyzed; we term this the dumping index (Figure 2H). Additionally, to control for potential fluctuations in aspirin concentration (i.e., solvent evaporation) and any inter-experiment variability, wild-type (*yw*) controls were included in each experiment. Using this approach, we would expect wild-type follicles to exhibit a dumping index of ~0.5, indicating half of the population of S10B follicles failed to complete nurse cell dumping in aspirin treated media. Experiments in which the wild-type dumping index was less than 0.4 or greater than 0.6 were excluded from further analyses. We observed an average dumping index of 0.505 (±0.054) for the inclusive data set of all wild-type controls (n=59). The raw data and calculations for two representative experiments – one for

an enhancer (*ena*^{210}/+) and one for a suppressor (*shg*^{E17B}/+) – are shown in Figure 2I. While the initial screen utilized one to two alleles and replicates per candidate, for those exhibiting a potential interaction additional alleles and/or replicates, along with factors implicated in interacting with or regulating them were tested. Here we present the aggregate data for all genotypes analyzed and their respective wild-type controls, including the number of trials (n), the average dumping index, and their standard deviation (SD, Table S1).

Identifying interactors

To aid in the identification of potential interactors in this screen, we wanted to focus on the differences in dumping index between wild-type control and experimental groups. To achieve this, we calculated the normalized experimental dumping indices for each experiment by subtracting the wild-type dumping index from the experimental dumping index (Figure 2H-I). Normalized dumping indices for each genotype were then averaged and plotted (Figure 3). By normalizing the data in this manner, the plotted values represent the net change in dumping index due to reduced levels of the factor tested. Positive values indicate that reduction of the factor tested suppressed sensitivity to COX inhibition (i.e. more follicles completed dumping), while negative values indicate enhanced sensitivity (i.e. less follicles completed dumping). The magnitude of this change indicates the relative strength of the observed suppression or enhancement. Using this strategy, we classified a number of genes falling into one of three categories: non-interactors, weak interactors, and strong interactors.

Based on this normalized data set, we defined non-interactors as any genotype that fails to exhibit a change in dumping index greater than one standard deviation away from wild-type values (±0.054; calculated from non-normalized aggregate wild-type controls). Factors falling into this category include both actin binding proteins and signaling pathway components known to play critical roles throughout *Drosophila* oogenesis, including: the formin Cappuccino; the actin cross-linking protein Kelch; the actin monomer binding protein Profilin (*Drosophila* Chickadee, Chic); the actin bundling protein Villin (*Drosophila* Quail); a TGFβ-like and BMP-like ligand Decapentaplegic (Dpp); and Abelson Tyrosine Kinase (Abl) (Figure 3 and Table S1).

It is important to note that a non-interactor may fail to interact because it is not regulated by PGs or because heterozygosity does not result in a sufficient enough reduction in protein to allow an interaction to be observed.

Genotypes exhibiting a change in dumping index between one and three standard deviations away from wild-type values were defined as weak interactors (between ±0.054 and ±0.162). Factors falling into this category include the small GTPase, Rho (*Drosophila* Rho-like, RhoL) and the Rho effector, Rho-associated Protein Kinase (ROCK, *Drosophila* ROK) (Figure 3 and Table S1).

Strong interactors were defined as any genotype exhibiting a change in dumping index equal to or greater than three standard deviations away from wild-type values (±0.162). Based on this definition, we identified a number of factors whose genetic reduction strongly sensitizes follicles to the effects of COX inhibition, including: the actin filament barbed end capper Cp; the actin elongation factor Ena; the contractile protein MRLC; and the actin bundling protein Fascin (Figure 3 and Table S1). Additionally, we uncovered two factors whose genetic reduction strongly suppresses follicle sensitivity to the effects of COX inhibition: the cell adhesion molecule E-Cadherin and the Enabled/Vasodilator-stimulated phosphoprotein (Ena/VASP) ligand Lamellipodin (Lpd, *Drosophila* Pico; Figure 3 and Table S1). Notably the strong and weak interactors represent actin binding proteins and related factors that participate in parallel actin bundle formation and nurse cell contractility – processes that fail when PG signaling is lost (Figure 1C-D; (TOOTLE AND SPRADLING 2008; GROEN *et al.* 2012; SPRACKLEN *et al.* 2014).

While all of the candidates uncovered in this screen are interesting, we chose to follow up on a subset of strong interactors. One such interactor is Fascin. Fascin is an actin bundling protein (reviewed in (EDWARDS AND BRYAN 1995) required for parallel actin filament bundle formation during S10B (CANT *et al.* 1994). Reduction of Fascin enhances sensitivity to COX inhibition (Figure 3 and Table S1). Through subsequent pharmacologic and genetic studies, we validated Fascin as a novel downstream target of PG signaling (GROEN *et al.* 2012). However, the mechanism(s) by which Fascin is regulated downstream of PG signaling remain poorly

understood. Recent studies indicate PGs regulate the subcellular localization of Fascin (GROEN *et al.* 2015; JAYO *et al.* 2016; KELPSCH *et al.* 2016). Additionally, it is likely that PGs control Fascin through post-translational modifications (Groen and Tootle, unpublished data). Here we present data for three strong interactors: Ena, Cp, and MRLC.

Heterozygosity for a localization defective Ena allele sensitizes follicles to COX inhibition

Ena, the sole *Drosophila* homolog of the Ena/VASP family of actin elongation factors (GERTLER *et al.* 1995), is a large protein containing multiple domains including: an Ena/VASP homology domain 1 (EVH1), responsible for mediating Ena localization; a glutamate-rich region; a proline-rich core; and an EVH2 domain, containing G- and F-actin binding sites and a tetramerization motif (Figure 4A). Like Fascin, Ena is required for parallel actin filament bundle formation during S10B (GATES *et al.* 2009).

To assess whether Ena is a downstream target of PG signaling during the actin remodeling that occurs during S10B, we asked if reduced Ena levels modified follicle sensitivity to COX inhibition. Here, we took advantage of six different *ena* alleles. These alleles included two well-characterized null alleles recovered from a gamma ray-induced mutagenesis screen (ena^{GC1} and ena^{GC5}, (GERTLER *et al.* 1995)), two alleles recovered from insertional mutagenesis screens that are predicted to be hypomorphic ($ena^{DG14706}$ (HUET *et al.* 2002) and $ena^{EY13131}$ (BELLEN *et al.* 2011)), and two well-characterized alleles recovered from an ethyl nitroso-urea mutagenesis screen (ena^{23} and ena^{210} (AHERN-DJAMALI *et al.* 1998)). The ena^{23} allele contains one missense mutation (N397F) of unknown functional consequence and a nonsense mutation (K636STOP) resulting in loss of the tetramerization motif within the EVH2 domain (Figure 4A;(AHERN-DJAMALI *et al.* 1998)). The ena^{210} allele contains a missense mutation (A97V) within the EVH1 domain (Figure 4A), which disrupts *in vitro* interaction between Ena and Zyxin, and likely alters Ena localization (AHERN-DJAMALI *et al.* 1998). All of the alleles except $ena^{EY13131}$ are homozygous lethal.

Using our pharmaco-genetic interaction screen, we find reduced levels of Ena result in an allele-dependent enhancement of follicle sensitivity to the effects of COX-inhibition. Heterozygosity for ena^{GC1} (0.417, ±0.013 SD, n=2), ena^{GC5} (0.6, n=1), $ena^{DG14706}$ (0.585, n=1), and ena^{23} (0.383, ±0.156 SD, n=5) or homozygosity for $ena^{EY13131}$ (0.423, ±0.084 SD, n=2) fails to significantly modify follicle sensitivity to COX inhibition compared to wild-type controls (0.467, ±0.049 SD, n=11) (Figure 4C). In contrast, heterozygosity for ena^{210}, the localization defective allele, strongly enhances follicle sensitivity to COX inhibition. Heterozygosity for ena^{210} results in a dumping index of 0.192 (±0.135 SD, n=5) compared to 0.467 (±0.049 SD, n=11) for wild-type controls (p=0.0003) (Figure 4C and Table S1).

While multiple alleles fail to show an interaction, the ena^{210} allele strongly enhances follicle sensitivity to COX inhibition in our pharmaco-genetic interaction screen. There are a number of potential explanations for this finding. It is possible that this allele-specific interaction could be due to genetic background effects that are specific to the ena^{210} allele. Given that the ena^{23} and ena^{210} alleles were generated in the same genetic background and have both been recombined onto the same FRT bearing chromosome, genetic background effects are unlikely to account for the observed differences. It is more likely the allele-specific interaction we observe is due to either the level of functional Ena or the nature of alleles tested. Our western blot analysis reveals that total Ena levels are similarly mildly reduced in ena^{GC1}, ena^{GC5}, $ena^{DG14706}$, ena^{23}, and ena^{210} heterozygotes and $ena^{EY13131}$ homozygotes (~80% of wild-type controls) (Figure 4B). Additionally, both the ena^{23} and ena^{210} alleles produce stable mutant protein products. Thus, heterozygosity for ena^{23}, and ena^{210} would be expected to result in a mixture of both wild-type and mutant protein; thus, reducing functional levels Ena further. Because the protein product encoded by ena^{23} lacks a tetramerization domain, we hypothesize heterozygosity for ena^{210} may result in a stronger effect on Ena function, as the mutant protein would be capable of forming tetramers with wild-type Ena.

The observation that heterozygosity for the ena^{210} allele strongly sensitizes follicles to the effects of COX inhibition suggests that PG signaling may regulate parallel actin filament

bundle formation during S10B, at least in part, by modulating Ena localization. Supporting this idea, using immunofluorescence and confocal microscopy we previously found Ena localization to the barbed ends of actin filament bundles at the nurse cell membranes during S10B is reduced in *pxt* mutants, compared to *wildtype* (SPRACKLEN *et al.* 2014). This qualitative reduction in localization is not due to altered Ena levels as Ena expression at either the mRNA (TOOTLE *et al.* 2011; SPRACKLEN *et al.* 2014) or protein level (SPRACKLEN *et al.* 2014) is unchanged in *pxt* mutants. Notably, the extent of the reduction in Ena localization corresponds to the severity of the S10B phenotype in *pxt* mutants, such that when there are nearly no actin filament bundles, there is similarly little to no Ena (SPRACKLEN *et al.* 2014). As Ena is required for bundle formation/elongation during S10B (GATES *et al.* 2009), we hypothesize the reduction in Ena localization to sites of bundle formation during S10B is one cause of the bundle defects observed in *pxt* mutants. Together these data suggest PG signaling may be required to promote appropriate Ena localization and/or activity during S10B. Exactly how this regulation is achieved remains unclear but is likely through post-translational mechanisms. One intriguing means by which PGs may regulate Ena activity is through controlling Fascin, a known downstream effector of PGs (GROEN *et al.* 2012; GROEN *et al.* 2015). Indeed, Fascin has be shown to promote Ena processivity, increasing filament elongation (WINKELMAN *et al.* 2014; HARKER *et al.* 2019).

To further explore the role of Ena as a putative downstream target of PG signaling during S10B, we assessed pharmaco-genetic interactions with two Ena interacting proteins – Abl and Lpd. Genetic studies originally implicated Abl as a negative regulator of Ena (GERTLER *et al.* 1990; GREVENGOED *et al.* 2003), and biochemical studies uncovered at least six tyrosines on Ena are phosphorylated by Abl (GERTLER *et al.* 1995; COMER *et al.* 1998). However, it remains unclear how phosphorylation affects Ena activity (BRADLEY AND KOLESKE 2009). More recent work suggests Abl may positively regulate Ena through Lpd. Lpd binds to Ena/VASP proteins and promotes actin elongation and cell migration (KRAUSE *et al.* 2004; HANSEN AND MULLINS 2015). In *Drosophila*, Lpd binds Ena and heterozygosity for the ena^{210} allele suppresses the defects due to Lpd overexpression (LYULCHEVA *et al.* 2008). Notably, Abl phosphorylates Lpd,

which promotes Lpd association with Ena/VASP proteins and other actin regulators (MICHAEL *et al.* 2010; CARMONA *et al.* 2016). Thus, Abl and Lpd are critical regulators of Ena activity. To begin to assess if PGs regulate Ena via Abl and/or Lpd we performed pharmaco-genetic interactions. Heterozygosity for abl^{4} does not alter follicle sensitivity to COX inhibition (Figure 3 and Table S1; dumping index of 0.414 compared to 0.506 for controls, n=4). This finding may be due to insufficient reduction of Abl necessary to see an interaction or may reflect that PGs do not regulate Abl. Based on a single trial, homozygosity for one *lpd* allele ($pico^{KG00685}$) suppresses follicle sensitivity to COX inhibition (Figure 3 and Table S1). As Lpd regulates the localization of Ena and other actin elongation factors (MICHAEL *et al.* 2010; CARMONA *et al.* 2016), and PGs regulate the localization of Ena (SPRACKLEN *et al.* 2014), we hypothesize that loss of PGs results in misregulation and mislocalization of Lpd and, thereby Ena. Thus, reducing Lpd may restore Ena localization.

Reduced Cp strongly sensitizes follicles to the effects of COX inhibition

Another means by which PGs could regulate Ena is via controlling Cp, a functional antagonist of Ena/VASP activity (BEAR *et al.* 2002; BEAR AND GERTLER 2009). Cp binds to the barbed ends of actin filaments and prevents their elongation by blocking the addition of actin monomers to the growing filament [reviewed in (COOPER AND SEPT 2008)]. Cp is a heterodimer composed of Capping protein α (Cpa; *Drosophila* Capping protein alpha, Cpa) and Capping protein β (Cpb; *Drosophila* Capping protein beta, Cpb). Additionally, Cp has been shown to play critical roles during *Drosophila* oogenesis, including oocyte determination (GATES *et al.* 2009), parallel actin filament bundle formation during S10B (GATES *et al.* 2009; OGIENKO *et al.* 2013), and border cell migration (GATES *et al.* 2009; LUCAS *et al.* 2013; OGIENKO *et al.* 2013).
With these findings in mind, we asked if reduced Cp could alter follicle sensitivity to COX inhibition using a lethal P-element insertional mutation in *cpa* ($cpa^{KG02261}$ (BELLEN *et al.* 2004)) and two EMS hypomorphic *cpb* alleles ($cpb^{6.15}$ and cpb^{F19} (HOPMANN *et al.* 1996)). Initially, we hypothesized that if reduced levels of Ena sensitized follicles to the effects of COX inhibition,

then reduction of a negative regulator of Ena activity would have an opposite effect, suppressing follicle sensitivity to COX inhibition. Surprisingly, we found heterozygosity for all alleles of *cpa* and *cpb* tested enhances follicle sensitivity to the effects of COX inhibition (Figure 4D). Heterozygosity for $cpa^{KG02261}$ results in a dumping index of 0.262 (±0.088 SD, n=3) compared to 0.486 (±0.026 SD, n=9) for wild-type controls (p=0.002). Heterozygosity for $cpb^{6.15}$ results in a dumping index of 0.313 (±0.148 SD, n=4; p=0.0068), and heterozygosity for cpb^{F19} results in a dumping index of 0.157 (±0.056 SD, n=3; p=<0.0001). These data reveal that reduced Cp enhances the effects of COX inhibition to block nurse cell dumping and follicle development.

Based on the *in vitro* antagonistic relationship between Ena and Cp, it seems surprising that reduction of either enhances the effects of COX inhibition. One possibility is that Cp acts on actin filaments generated by other elongation factors. However, Ena is the only elongation factor implicated in regulating bundle formation necessary for nurse cell dumping (GATES *et al.* 2009). Thus, we favor the model that the primary role of Cp during S10B is to modulate Ena. Loss of Ena and loss of Cp were previously shown to result in similar, but subtly different phenotypes during S10B of oogenesis (GATES *et al.* 2009). Specifically, loss of either Ena or Cp results in loss of nurse cell cortical actin integrity and leads to impaired nurse cell dumping due to parallel actin filament bundle formation defects (GATES *et al.* 2009). Whereas loss of Ena results in a substantial decrease in the number of cytoplasmic actin bundles formed during S10B, loss of Cp severely disrupts the organization/distribution of the bundles, but not their overall number (GATES *et al.* 2009). Based on their data, Gates *et al*. reasoned that capping/anti-capping activity must be carefully balanced to promote appropriate cytoplasmic actin filament bundle formation during S10B (GATES *et al.* 2009). Our findings suggest PG signaling may play a role in regulating this balance, thereby promoting appropriate parallel actin filament bundle formation during oogenesis.

Reduced MRLC strongly sensitizes follicles to the effects of COX inhibition

Non-muscle myosin II mediates the contraction of actin filaments and is composed of two copies of three subunits: Myosin Heavy Chain (*Drosophila* Zipper, Zip), Myosin Essential Light Chain (*Drosophila* Mlc-c), and MRLC (*Drosophila* Spaghetti squash, Sqh). Phosphorylation of MRLC by Rho kinase (ROCK) and Myosin Light Chain Kinase (MLCK) activates myosin (DIAZ *et al.* 2009; VICENTE-MANZANARES *et al.* 2009). MRLC inactivation is achieved by dephosphorylation via Myosin Phosphatase (MYPT; *Drosophila* Mbs and Flw; (GRASSIE *et al.* 2011)).

The pharmaco-genetic interaction screen identified MRLC as a strong enhancer of follicle sensitivity to COX inhibition. We tested three MRLC alleles. sqh^{AX3} is a null allele derived from a 5kb genomic deletion removing most of the *sqh* locus (JORDAN AND KARESS 1997). $sqh^{EY09875}$ is the result of a P-element insertion upstream of the *sqh* translation start site (BELLEN *et al.* 2004). We also tested a large chromosomal deficiency, Df(1)5D, that removes 51 loci, including *sqh*. As expected, all three alleles are homozygous lethal. In our assay, we find heterozygosity for *sqh* enhances follicle sensitivity to COX inhibition, with heterozygosity for sqh^{AX3} resulting in a dumping index of 0.266 (±0.072 SD, n=3; p=0.067), heterozygosity for $sqh^{EY09875}$ resulting in a dumping index of 0.294 (±0.159 SD, n=4; p=0.076), and heterozygosity for *DF(1)5D* resulting in a dumping index of 0.374 (±0.255 SD, n=3; p=0.43) (Figure 5A). These data suggest PGs normally promote MRLC activity. MRLC is required for nurse cell contraction during S11, as germline loss of MRLC blocks nurse cell dumping but does not cause actin bundle defects (WHEATLEY *et al.* 1995). While loss of Pxt causes severe actin bundle defects, unlike other mutants lacking actin bundles (such as *fascin* mutants, Figure 1F), the nurse cell nuclei do not plug the ring canals; this finding indicates that contraction fails in the absence of Pxt (Figure 1D compared to F; (TOOTLE AND SPRADLING 2008; GROEN *et al.* 2012)). Given the pharmaco-genetic interaction, we hypothesize PGs activate MRLC to drive nurse cell contraction required for nurse cell dumping.

To explore this idea further, we assessed how loss of Pxt affects the level and activity of non-muscle Myosin II. While immunoblotting for MRLC was unsuccessful, immunoblots for Zipper, the *Drosophila* Myosin Heavy Chain, reveal that non-muscle Myosin II levels are unchanged when PGs are lost (Figure 5B). Next, we examined MRLC by immunofluorescence (MAJUMDER *et al.* 2012; ARANJUEZ *et al.* 2016); MRLC localization is dependent on its activation by phosphorylation (VICENTE-MANZANARES *et al.* 2009). During S10B, active MRLC is enriched at the nurse cell membranes, with the strongest staining in the posterior nurse cells (Figure 5C-C'). When Pxt is lost, active MRLC no longer exhibits the posterior enrichment and has a patchy appearance at the nurse cell membranes (Figure 5D-D'). This difference is not due to cortical actin defects, as phalloidin-labeled cortical F-actin is present in areas of low active MRLC in *pxt* mutants (Figure 5D" compared to C"). To quantify the difference in active MRLC, average fluorescence intensity was measured along a segment of a posterior nurse cell membrane. Loss of Pxt by two different alleles results in a significant decrease in the average fluorescent intensity of active MRLC (Figure 5E, $p<0.0001$). These data suggest PGs regulate non-muscle Myosin II activity to mediate nurse cell contractility.

Conclusion

The results of this pharmaco-genetic interaction screen support a model in which PG signaling regulates the localization and/or activity of multiple actin binding proteins to coordinate the actin remodeling events during S10B-11 that are required for female fertility. Specifically, our data reveal a number of factors known to both regulate parallel actin filament bundle formation and structure, and to promote nurse cell contractility as new downstream targets of PG signaling during *Drosophila* oogenesis.

Parallel actin filament bundle formation during S10B requires the activity of numerous actin binding proteins, including Profilin (COOLEY *et al.* 1992), Fascin (CANT *et al.* 1994), Ena (GATES *et al.* 2009), Cp (GATES *et al.* 2009; OGIENKO *et al.* 2013), and Villin (MAHAJAN-MIKLOS AND COOLEY 1994). Reduced levels of Fascin, Ena, and Cp strongly sensitize S10B follicles to the effects of COX inhibition (Figures 3-4 and Table S1). However, not all proteins

required for parallel actin filament bundle formation during S10B exhibit an interaction in our pharmaco-genetic interaction screen, as reduced levels of Villin (GROEN *et al.* 2012) or Profilin fail to modify follicle sensitivity to COX inhibition (Figure 3 and Table S1). These data suggest PG signaling regulates a specific subset of actin binding proteins to promote actin filament bundle formation during *Drosophila* oogenesis.

In addition to promoting actin filament bundle formation during S10B, our data also suggest PG signaling is required to promote nurse cell contractility during S11. During nurse cell dumping (S11), the contractile force required to transfer the nurse cell cytoplasm to the oocyte is generated through non-muscle Myosin II-dependent contraction of the nurse cell cortical actin (WHEATLEY *et al.* 1995). Reduced levels of MRLC strongly enhance follicle sensitivity to the effects of COX inhibition and loss of Pxt results in decreased active MRLC at the nurse cell membranes (Figures 3, 5 and Table S1). Additionally, ROCK, which is known to promote non-muscle Myosin II activity through phosphorylation of both the MRLC and Myosin Light Chain Phosphatase (AMANO *et al.* 1996), mildly sensitizes follicles to the effects of COX inhibition (Figure 3 and Table S1). Together, these data are consistent with a model in which PG signaling is required during nurse cell dumping to promote nurse cell contractility through positive regulation of non-muscle Myosin II activity.

Future studies are required to elucidate the molecular mechanisms by which PG signaling regulates the localization/activity of the actin regulators uncovered in this screen. These same mechanisms are likely conserved in higher species. Indeed, both increased PG production (ROLLAND *et al.* 1980; CHEN *et al.* 2001; KHURI *et al.* 2001; GALLO *et al.* 2002; DENKERT *et al.* 2003; ALLAJ *et al.* 2013) and actin binding protein expression (YAMAGUCHI AND CONDEELIS 2007; GROSS 2013; IZDEBSKA *et al.* 2018) are associated with increased invasiveness and poor prognosis in multiple human cancers. Given our screen findings, we speculate that PG signaling regulates actin dynamics to drive cancer progression and this is an important area for future investigation.

ACKNOWLEDGMENTS

We thank Stephanie Meyer for her extensive contributions to the screen as an undergraduate researcher, and George Aranjuez and Jocelyn McDonald for the protocol for immunostaining *Drosophila* follicles for active MRLC. We thank the members of the Tootle Lab for helpful discussions and careful review of the manuscript. A.J.S. was supported by the National Institutes of Health (NIH) Predoctoral Training Grant in Pharmacological Sciences T32GM067795, NIH Postdoctoral Training Grant in Integrated Training in Cancer Model Systems T32CA009156, and NIH Ruth L. Kirschstein National Research Service Award Individual Postdoctoral Fellowship F32GM117803. M.C.L. is supported, in part, by the University of Iowa, Graduate College Summer Fellowship, and has previously been supported by the Anatomy and Cell Biology Department Graduate Fellowship. This work was supported by National Science Foundation grant MCB-115827 and NIH grant GM116885 to T.L.T.

Figure Legends:

Figure 1: Pxt is required for actin remodeling during S10B and cellular contraction during S11. A-F. Maximum projection images of 2-4 confocal slices of S10B and S11 follicles of the indicated genotypes. Stage was determined in the mutants by centripetal follicle cell migration. DAPI (cyan) and phalloidin (white). Scale bars=50μm. A-B. *wild-type*. C-D $pxt^{f/f}$. E-F. $fascin^{sn28/sn28}$. Yellow arrowheads indicate nurse cell nuclei that have plugged the ring canals during dumping. Loss of Pxt results in failure of nurse cell dumping, follicles fail to properly form actin bundles (C) in the nurse cells and don't undergo nurse cell contraction (D). Conversely, while loss of Fascin results in a lack of actin bundles (E) in the nurse cells, follicles still undergo contraction as evident by nurse cell nuclei plugging the ring canals (F, yellow arrowheads).

Figure 2. In vitro egg maturation examples and screen rationale. A. Representative images of S10B-S14 *Drosophila* follicles taken using a stereo dissecting scope; anterior is at the left. Blue asterisks indicate the oocyte, yellow brackets mark the nurse cells, and the white arrow indicates the dorsal appendages in S14. In the IVEM assay, follicles that remain in S10B-11 are scored as having failed to dump, whereas follicles that have reached S12-14 are scored as having completed dumping. B-F. Representative images of in vitro maturing follicles at the start (B) or end of the experiment (C-F) in control media (B-C, vehicle) or aspirin media (D-F, IC_{50} aspirin). Follicles failing to dump are marked with red asterisks. G. Diagrams illustrating the rationale behind the pharmaco-genetic interaction screen. H. Formulas for calculating the dumping index and normalized dumping index (the colors match the data in the table in I). I. Table of the data and example calculations from two experiments – one for an enhancer (ena^{210}) and one for a suppressor (shg^{E17B}). In control media, the majority of wild-type follicles complete nurse cell dumping (C, 92%), while in aspirin media only 50% complete dumping (D, G). The dumping index for control follicles is expected to be around 0.5 (G, I). A genetic enhancer will result in

<50% completing dumping in aspirin media (E [23%] and G), a dumping index of <0.5, and a negative normalized dumping index (I, *ena*^{210}). A genetic suppressor will result in >50% completing dumping (F [73%] and G), a dumping index of >0.5, and a positive normalized dumping index (I, s*hg*^{E17B}). Reduced levels of an actin-binding protein that is not a downstream target of PG signaling during S10B would not be expected to modify follicle sensitivity to COX inhibition, resulting in 50% completing dumping (G), a dumping index of ~0.5, and a normalized dumping index of ~0. Scale bars = 50μm.

Figure 3. Pharmaco-genetic interaction screen reveals multiple actin- binding proteins as candidate downstream targets of prostaglandin signaling. Chart of the normalized dumping indices for all genotypes tested in the first pass of the pharmaco-genetic interaction screen. Wild-type control values were set to zero and normalized experimental dumping indices were calculated by subtracting the dumping index of the experimental group from the wild-type dumping index for each individual experiment (see Figure 2H). Dashed red lines indicate ±1 standard deviation (±0.054) from all wild-type control values. Solid red lines represent ±3 standard deviations (±0.162) from all wild-type control values. Genotypes exhibiting normalized dumping indices between 0 and ±1 standard deviation from wild-type control values are classified as non-interactors. Genotypes exhibiting normalized dumping indices falling between ±1 to ±3 standard deviations from wild-type control values are classified as weak interactors. Genotypes exhibiting normalized dumping indices falling outside of ±3 standard deviations from wild-type control values are classified as strong interactors. Error bars = standard deviation (SD).

Figure 4. Altering Ena activity strongly sensitized S10B follicles to the effects of COX inhibition. A. Schematic detailing Ena protein structure and the mutations carried by the *ena*^{23} and *ena*^{210} alleles. EVH=Ena/VASP homology domain; G= G-actin binding domain, F= F-actin binding domain, T= tetramerization domain. B. Representative western blot and quantification of Ena levels for genotypes indicated. C. Graph of pharmaco-genetic interaction data for *ena*

alleles. D. Graph of pharmaco-interaction data for *cp* alleles. Heterozygosity for ena^{23}, ena^{210}, ena^{GC1}, ena^{GC5}, or $ena^{DG14706}$ or homozygosity for $ena^{EY13131}$ results in a mild decrease in total Ena levels compared to wild-type controls (B, n=2, error bars = SD; note both full-length and truncated Ena are observed in the ena^{23}/+ lane). Additionally, heterozygosity for an Ena duplication (*ena* dup; Dp(2;2)Cam18/+) results in a mild increase in total Ena levels compared to wild-type controls (B). Heterozygosity for ena^{GC1}, ena^{GC5}, $ena^{DG14706}$, and ena^{23}, as well as homozygosity $ena^{EY13131}$, fail to modify follicle sensitivity to the effects of COX inhibition (C). However, heterozygosity for the ena^{210} allele significantly enhances the ability of 1.5mM aspirin to inhibit nurse cell dumping compared to wild-type controls (C). Heterozygosity the alpha-subunit of Capping protein ($cpa^{KG02261}$), and the beta-subunit of Capping protein ($cpb^{6.15}$ and cpb^{F19}) significantly enhance the ability of 1.5mM aspirin to block nurse cell dumping compared to wild-type controls (D). The number of trials (n) are indicated in Table S1. Error bars = SD. **** $p < 0.0001$, *** $p < 0.001$, ** $p < 0.01$, and * $p < 0.05$.

Figure 5. PGs pharmaco-genetically interact with and regulate the activity of MRLC. A. Graph of pharmaco-interaction data for *sqh* alleles; *sqh* encodes the *Drosophila* MRLC. B. Representative western blot and quantification of Zipper (*Drosophila* MHC) levels for genotypes indicated. Tubulin was used as a loading control and Zipper protein levels were normalized to Tubulin. C-D". Maximum projections of 2-3 confocal slices of S10 follicles of the indicated genotypes. C, D. Phosphorylated myosin regulatory light chain (S19), white. C', D'. Phosphorylated myosin regulatory light chain (S19) pseudocolored with Rainbow RGB, red indicating the highest intensity pixels. Insets are zoom-ins of the nurse cell membranes within the yellow squares. C'', D''. Phalloidin (F-actin), white. E. Graph showing quantification of p-MRLC intensity in arbitrary units (AU) along the membrane of a posterior nurse cell of a S10B follicle of the indicated genotypes. Briefly, the average fluorescent intensity of p-MRLC was measured for the same length along a posterior nurse cell membrane for each of the indicated genotypes; each circle represents a single follicle. Heterozygosity for sqh^{AX3} or $sqh^{EY09875}$

enhances the ability of aspirin to inhibit nurse cell dumping compared to wild-type controls, and heterozygosity for $sqh^{Df(1)5D}$ results in a mild increase in aspirin's ability to inhibit nurse cell dumping (A). Loss of PG signaling using two different Pxt alleles, $pxt^{EY/EY}$ or $pxt^{f/f}$, does not alter total Zipper (*Drosophila* MHC) levels (B; n=3, error bars = SD). Loss of PG signaling alters phospho-MRLC localization on nurse cell membranes with the *pxt* mutants exhibiting patchy localization on throughout the follicle and aberrant enrichment on the anterior nurse cells (C-D'). The change in phospho-MRLC is not due to cortical actin breakdown, as the cortical actin is intact in the *pxt* mutant (C'', D''). Loss of Pxt results in reduced activated MRLC along the posterior nurse cell membranes (E). Error bars = SD. ns = $p>0.05$ and **** $p<0.0001$. Scale bars= 50μm.

References

Abramoff, M. D., P. J. Magalhaes and S. J. Ram, 2004 Image Processing with ImageJ. Biophotonics International 11**:** 36-42.

Ahern-Djamali, S. M., A. R. Comer, C. Bachmann, A. S. Kastenmeier, S. K. Reddy *et al.*, 1998 Mutations in Drosophila enabled and rescue by human vasodilator-stimulated phosphoprotein (VASP) indicate important functional roles for Ena/VASP homology domain 1 (EVH1) and EVH2 domains. Mol Biol Cell 9**:** 2157-2171.

Allaj, V., C. Guo and D. Nie, 2013 Non-steroid anti-inflammatory drugs, prostaglandins, and cancer. Cell Biosci 3**:** 8.

Amano, M., M. Ito, K. Kimura, Y. Fukata, K. Chihara *et al.*, 1996 Phosphorylation and activation of myosin by Rho-associated kinase (Rho-kinase). J Biol Chem 271**:** 20246-20249.

Aranjuez, G., A. Burtscher, K. Sawant, P. Majumder and J. A. McDonald, 2016 Dynamic myosin activation promotes collective morphology and migration by locally balancing oppositional forces from surrounding tissue. Mol Biol Cell 27**:** 1898-1910.

Aszodi, A., A. Pfeifer, M. Ahmad, M. Glauner, X. H. Zhou *et al.*, 1999 The vasodilator-stimulated phosphoprotein (VASP) is involved in cGMP- and cAMP-mediated inhibition of agonist-induced platelet aggregation, but is dispensable for smooth muscle function. EMBO Journal 18**:** 37-48.

Banan, A., G. S. Smith, E. R. Kokoska and T. A. Miller, 2000 Role of actin cytoskeleton in prostaglandin-induced protection against ethanol in an intestinal epithelial cell line. The Journal of surgical research 88**:** 104-113.

Bear, J. E., and F. B. Gertler, 2009 Ena/VASP: towards resolving a pointed controversy at the barbed end. J Cell Sci 122**:** 1947-1953.

Bear, J. E., T. M. Svitkina, M. Krause, D. A. Schafer, J. J. Loureiro *et al.*, 2002 Antagonism between Ena/VASP proteins and actin filament capping regulates fibroblast motility. 109**:** 509-521.

Bearer, E. L., J. M. Prakash and Z. Li, 2002 Actin dynamics in platelets. International Review of Cytology 217**:** 137-182.

Bellen, H. J., R. W. Levis, Y. He, J. W. Carlson, M. Evans-Holm *et al.*, 2011 The Drosophila gene disruption project: progress using transposons with distinctive site specificities. Genetics 188**:** 731-743.

Bellen, H. J., R. W. Levis, G. Liao, Y. He, J. W. Carlson *et al.*, 2004 The BDGP gene disruption project: single transposon insertions associated with 40% of Drosophila genes. Genetics 167**:** 761-781.

Birukova, A. A., T. Zagranichnaya, P. Fu, E. Alekseeva, W. Chen *et al.*, 2007 Prostaglandins PGE(2) and PGI(2) promote endothelial barrier enhancement via PKA- and Epac1/Rap1-dependent Rac activation. Experimental Cell Research 313**:** 2504-2520.

Bradley, W. D., and A. J. Koleske, 2009 Regulation of cell migration and morphogenesis by Abl-family kinases: emerging mechanisms and physiological contexts. J Cell Sci 122**:** 3441-3454.

Bulin, C., U. Albrecht, J. G. Bode, A. A. Weber, K. Schror *et al.*, 2005 Differential effects of vasodilatory prostaglandins on focal adhesions, cytoskeletal architecture, and migration in human aortic smooth muscle cells. Arteriosclerosis, Thrombosis, and Vascular Biology 25**:** 84-89.

Cant, K., B. A. Knowles, M. S. Mooseker and L. Cooley, 1994 Drosophila singed, a fascin homolog, is required for actin bundle formation during oogenesis and bristle extension. The Journal of cell biology 125**:** 369-380.

Carmona, G., U. Perera, C. Gillett, A. Naba, A. L. Law *et al.*, 2016 Lamellipodin promotes invasive 3D cancer cell migration via regulated interactions with Ena/VASP and SCAR/WAVE. Oncogene 35**:** 5155-5169.

Chen, W. S., S. J. Wei, J. M. Liu, M. Hsiao, J. Kou-Lin *et al.*, 2001 Tumor invasiveness and liver metastasis of colon cancer cells correlated with cyclooxygenase-2 (COX-2) expression and inhibited by a COX-2-selective inhibitor, etodolac. Int J Cancer 91**:** 894-899.

Comer, A. R., S. M. Ahern-Djamali, J. L. Juang, P. D. Jackson and F. M. Hoffmann, 1998 Phosphorylation of Enabled by the Drosophila Abelson tyrosine kinase regulates the in vivo function and protein-protein interactions of Enabled. Mol Cell Biol 18**:** 152-160.

Cooley, L., E. Verheyen and K. Ayers, 1992 chickadee encodes a profilin required for intercellular cytoplasm transport during Drosophila oogenesis. Cell 69**:** 173-184.

Cooper, J. A., and D. Sept, 2008 New insights into mechanism and regulation of actin capping protein. Int Rev Cell Mol Biol 267**:** 183-206.

Denkert, C., K. J. Winzer, B. M. Muller, W. Weichert, S. Pest *et al.*, 2003 Elevated expression of cyclooxygenase-2 is a negative prognostic factor for disease free survival and overall survival in patients with breast carcinoma. Cancer 97**:** 2978-2987.

Diaz, D., J. Valero, C. Airado, F. C. Baltanas, E. Weruaga *et al.*, 2009 Sexual dimorphic stages affect both proliferation and serotonergic innervation in the adult rostral migratory stream. Exp Neurol 216**:** 357-364.

Dormond, O., M. Bezzi, A. Mariotti and C. Ruegg, 2002 Prostaglandin E2 promotes integrin alpha Vbeta 3-dependent endothelial cell adhesion, rac-activation, and spreading through cAMP/PKA-dependent signaling. J Biol Chem 277**:** 45838-45846.

Edwards, R. A., and J. Bryan, 1995 Fascins, a family of actin bundling proteins. Cell Motil Cytoskeleton 32**:** 1-9.

Gallo, O., E. Masini, B. Bianchi, L. Bruschini, M. Paglierani *et al.*, 2002 Prognostic significance of cyclooxygenase-2 pathway and angiogenesis in head and neck squamous cell carcinoma. Hum Pathol 33**:** 708-714.

Gates, J., S. H. Nowotarski, H. Yin, J. P. Mahaffey, T. Bridges *et al.*, 2009 Enabled and Capping protein play important roles in shaping cell behavior during Drosophila oogenesis. Developmental Biology 333**:** 90-107.

Gertler, F. B., A. R. Comer, J. L. Juang, S. M. Ahern, M. J. Clark *et al.*, 1995 enabled, a dosage-sensitive suppressor of mutations in the Drosophila Abl tyrosine kinase, encodes an Abl substrate with SH3 domain-binding properties. Genes Dev 9**:** 521-533.

Gertler, F. B., J. S. Doctor and F. M. Hoffmann, 1990 Genetic suppression of mutations in the Drosophila abl proto-oncogene homolog. Science 248**:** 857-860.

Grassie, M. E., L. D. Moffat, M. P. Walsh and J. A. MacDonald, 2011 The myosin phosphatase targeting protein (MYPT) family: a regulated mechanism for achieving substrate specificity of the catalytic subunit of protein phosphatase type 1delta. Arch Biochem Biophys 510**:** 147-159.

Grevengoed, E. E., D. T. Fox, J. Gates and M. Peifer, 2003 Balancing different types of actin polymerization at distinct sites: roles for Abelson kinase and Enabled. J Cell Biol 163**:** 1267-1279.

Groen, C. M., A. Jayo, M. Parsons and T. L. Tootle, 2015 Prostaglandins regulate nuclear localization of Fascin and its function in nucleolar architecture. Mol Biol Cell 26**:** 1901-1917.

Groen, C. M., A. J. Spracklen, T. N. Fagan and T. L. Tootle, 2012 Drosophila Fascin is a novel downstream target of prostaglandin signaling during actin remodeling. Mol Biol Cell 23**:** 4567-4578.

Gross, S. R., 2013 Actin binding proteins: their ups and downs in metastatic life. Cell Adh Migr 7**:** 199-213.

Guild, G. M., P. S. Connelly, M. K. Shaw and L. G. Tilney, 1997 Actin filament cables in Drosophila nurse cells are composed of modules that slide passively past one another during dumping. The Journal of cell biology 138**:** 783-797.

Halbrugge, M., C. Friedrich, M. Eigenthaler, P. Schanzenbacher and U. Walter, 1990 Stoichiometric and reversible phosphorylation of a 46-kDa protein in human platelets in response to cGMP- and cAMP-elevating vasodilators. Journal of Biological Chemistry 265**:** 3088-3093.

Hansen, S. D., and R. D. Mullins, 2015 Lamellipodin promotes actin assembly by clustering Ena/VASP proteins and tethering them to actin filaments. Elife 4.
Harker, A. J., H. H. Katkar, T. C. Bidone, F. Aydin, G. A. Voth *et al.*, 2019 Ena/VASP processive elongation is modulated by avidity on actin filaments bundled by the filopodia cross-linker fascin. Mol Biol Cell 30**:** 851-862.
Hopmann, R., J. A. Cooper and K. G. Miller, 1996 Actin organization, bristle morphology, and viability are affected by actin capping protein mutations in Drosophila. J Cell Biol 133**:** 1293-1305.
Hudson, A. M., and L. Cooley, 2002 Understanding the function of actin-binding proteins through genetic analysis of Drosophila oogenesis. Annu Rev Genet 36**:** 455-488.
Huelsmann, S., J. Ylanne and N. H. Brown, 2013 Filopodia-like Actin Cables Position Nuclei in Association with Perinuclear Actin in Drosophila Nurse Cells. Dev Cell 26**:** 604-615.
Huet, F., J. T. Lu, K. V. Myrick, L. R. Baugh, M. A. Crosby *et al.*, 2002 A deletion-generator compound element allows deletion saturation analysis for genomewide phenotypic annotation. Proc Natl Acad Sci U S A 99**:** 9948-9953.
Izdebska, M., W. Zielinska, D. Grzanka and M. Gagat, 2018 The Role of Actin Dynamics and Actin-Binding Proteins Expression in Epithelial-to-Mesenchymal Transition and Its Association with Cancer Progression and Evaluation of Possible Therapeutic Targets. Biomed Res Int 2018**:** 4578373.
Jayo, A., M. Malboubi, S. Antoku, W. Chang, E. Ortiz-Zapater *et al.*, 2016 Fascin Regulates Nuclear Movement and Deformation in Migrating Cells. Dev Cell 38**:** 371-383.
Jordan, P., and R. Karess, 1997 Myosin light chain-activating phosphorylation sites are required for oogenesis in Drosophila. J Cell Biol 139**:** 1805-1819.
Kawada, N., H. Klein and K. Decker, 1992 Eicosanoid-mediated contractility of hepatic stellate cells. Biochem J 285 (Pt 2)**:** 367-371.
Kelpsch, D. J., C. M. Groen, T. N. Fagan, S. Sudhir and T. L. Tootle, 2016 Fascin regulates nuclear actin during Drosophila oogenesis. Mol Biol Cell 27**:** 2965-2979.
Khuri, F. R., H. Wu, J. J. Lee, B. L. Kemp, R. Lotan *et al.*, 2001 Cyclooxygenase-2 overexpression is a marker of poor prognosis in stage I non-small cell lung cancer. Clin Cancer Res 7**:** 861-867.
Krause, M., J. D. Leslie, M. Stewart, E. M. Lafuente, F. Valderrama *et al.*, 2004 Lamellipodin, an Ena/VASP ligand, is implicated in the regulation of lamellipodial dynamics. Dev Cell 7**:** 571-583.
Lucas, E. P., I. Khanal, P. Gaspar, G. C. Fletcher, C. Polesello *et al.*, 2013 The Hippo pathway polarizes the actin cytoskeleton during collective migration of Drosophila border cells. J Cell Biol 201**:** 875-885.
Lyulcheva, E., E. Taylor, M. Michael, A. Vehlow, S. Tan *et al.*, 2008 Drosophila pico and its mammalian ortholog lamellipodin activate serum response factor and promote cell proliferation. Dev Cell 15**:** 680-690.
Mahajan-Miklos, S., and L. Cooley, 1994 The villin-like protein encoded by the Drosophila quail gene is required for actin bundle assembly during oogenesis. Cell 78**:** 291-301.
Majumder, P., G. Aranjuez, J. Amick and J. A. McDonald, 2012 Par-1 controls myosin-II activity through myosin phosphatase to regulate border cell migration. Curr Biol 22**:** 363-372.
Martineau, L. C., L. I. McVeigh, B. J. Jasmin and C. R. Kennedy, 2004 p38 MAP kinase mediates mechanically induced COX-2 and PG EP4 receptor expression in podocytes: implications for the actin cytoskeleton. Am J Physiol Renal Physiol 286**:** F693-701.
Michael, M., A. Vehlow, C. Navarro and M. Krause, 2010 c-Abl, Lamellipodin, and Ena/VASP proteins cooperate in dorsal ruffling of fibroblasts and axonal morphogenesis. Curr Biol 20**:** 783-791.
Nolte, C., M. Eigenthaler, P. Schanzenbacher and U. Walter, 1991 Comparison of vasodilatory prostaglandins with respect to cAMP-mediated phosphorylation of a target substrate in intact human platelets. Biochemical Pharmacology 42**:** 253-262.

Ogienko, A. A., D. A. Karagodin, V. V. Lashina, S. I. Baiborodin, E. S. Omelina *et al.*, 2013 Capping protein beta is required for actin cytoskeleton organisation and cell migration during Drosophila oogenesis. Cell Biol Int 37**:** 149-159.

Peppelenbosch, M. P., L. G. Tertoolen, W. J. Hage and S. W. de Laat, 1993 Epidermal growth factor-induced actin remodeling is regulated by 5-lipoxygenase and cyclooxygenase products. Cell 74**:** 565-575.

Pierce, K. L., H. Fujino, D. Srinivasan and J. W. Regan, 1999 Activation of FP prostanoid receptor isoforms leads to Rho-mediated changes in cell morphology and in the cell cytoskeleton. J Biol Chem 274**:** 35944-35949.

Rolland, P. H., P. M. Martin, J. Jacquemier, A. M. Rolland and M. Toga, 1980 Prostaglandin in human breast cancer: Evidence suggesting that an elevated prostaglandin production is a marker of high metastatic potential for neoplastic cells. J Natl Cancer Inst 64**:** 1061-1070.

Spracklen, A. J., D. J. Kelpsch, X. Chen, C. N. Spracklen and T. L. Tootle, 2014 Prostaglandins temporally regulate cytoplasmic actin bundle formation during Drosophila oogenesis. Mol Biol Cell 25**:** 397-411.

Spracklen, A. J., and T. L. Tootle, 2013 The Utility of Stage-specific Mid-to-late Drosophila Follicle Isolation. J Vis Exp.

Spracklen, A. J., and T. L. Tootle, 2015 Drosophila – a model for studying prostaglandin signaling., pp. 181-197 in *Bioactive Lipid Mediators: Current Reviews and Protocols.*, edited by T. Yokomizo and M. Murakami. Springer Protocols.

Tootle, T. L., 2013 Genetic insights into the in vivo functions of prostaglandin signaling. Int J Biochem Cell Biol.

Tootle, T. L., and A. C. Spradling, 2008 Drosophila Pxt: a cyclooxygenase-like facilitator of follicle maturation. Development 135**:** 839-847.

Tootle, T. L., D. Williams, A. Hubb, R. Frederick and A. Spradling, 2011 Drosophila eggshell production: identification of new genes and coordination by Pxt. PLoS One 6**:** e19943.

Vicente-Manzanares, M., X. Ma, R. S. Adelstein and A. R. Horwitz, 2009 Non-muscle myosin II takes centre stage in cell adhesion and migration. Nat Rev Mol Cell Biol 10**:** 778-790.

Wheatley, S., S. Kulkarni and R. Karess, 1995 Drosophila nonmuscle myosin II is required for rapid cytoplasmic transport during oogenesis and for axial nuclear migration in early embryos. Development 121**:** 1937-1946.

Winkelman, J. D., C. G. Bilancia, M. Peifer and D. R. Kovar, 2014 Ena/VASP Enabled is a highly processive actin polymerase tailored to self-assemble parallel-bundled F-actin networks with Fascin. Proc Natl Acad Sci U S A 111**:** 4121-4126.

Yamaguchi, H., and J. Condeelis, 2007 Regulation of the actin cytoskeleton in cancer cell migration and invasion. Biochim Biophys Acta 1773**:** 642-652.

S10B

S11

wild-type

A

B

DAPI Phalloidin

pxt-/-

C

D

fascin-/-

E

F

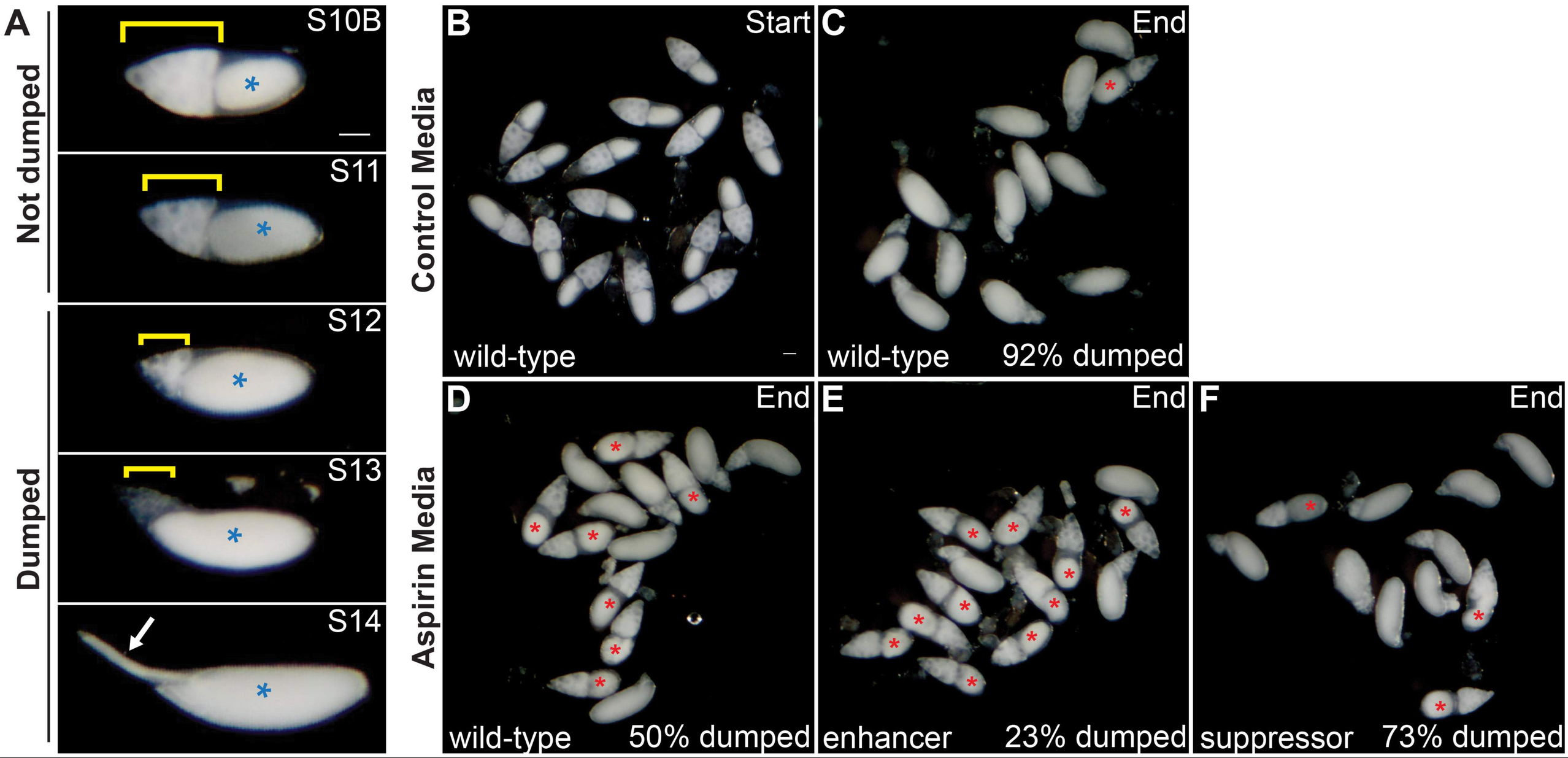

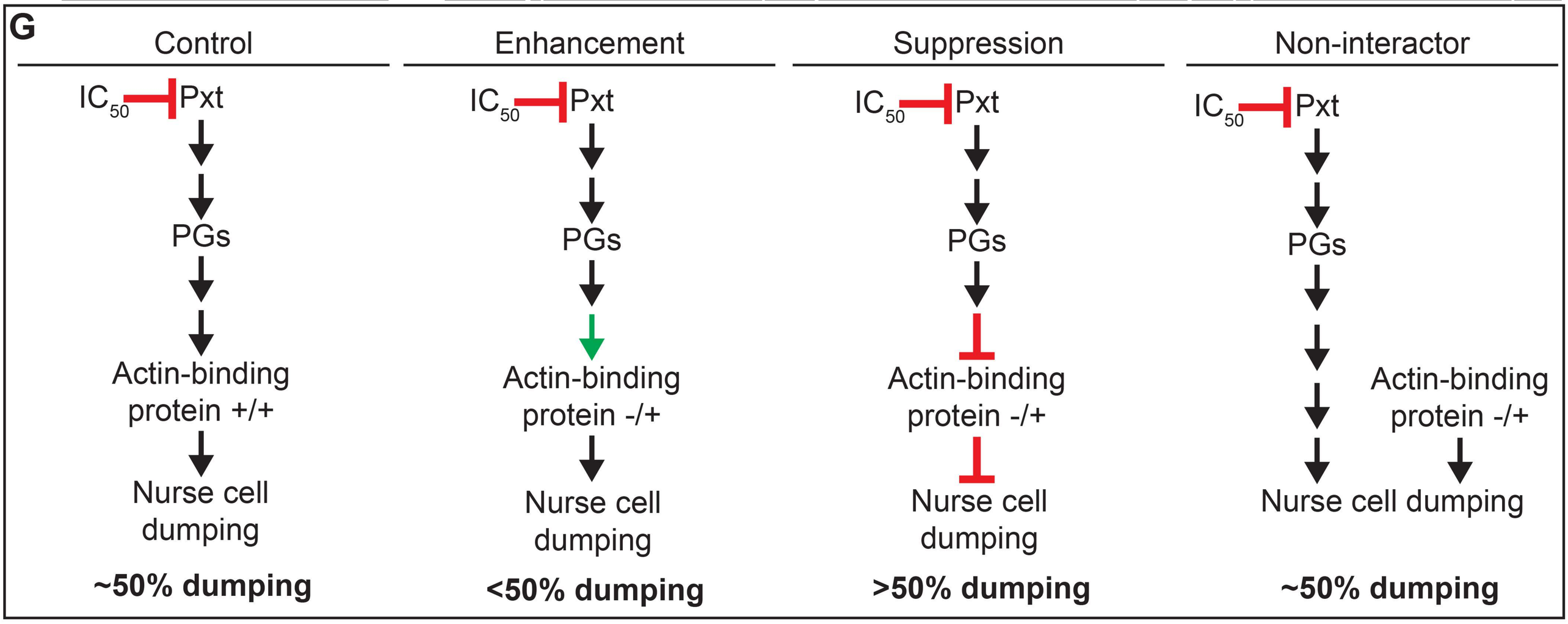

H

Dumping Index =

$$\frac{\text{\% dumping in 1.5mM Aspirin}}{\text{\% dumping in control media}}$$

Normalized Dumping Index =

Experimental dumping index − Control dumping index

I

Genotype	Aspirin	# follicles dumped	Total follicles	% dumped	Dumping index	Normalized dumping index
Control	-	17	17	100	50/100=0.50	0.36-0.50=-0.14
Control	+	10	20	50		
ena^{210}/+	-	14	18	78	28/78=0.36	
ena^{210}/+	+	5	18	28		
Control	-	24	28	86	46/86=0.53	0.78-0.53=0.25
Control	+	14	28	46		
shg^{E17B}/+	-	22	25	88	69/88=0.78	
shg^{E17B}/+	+	18	26	69		

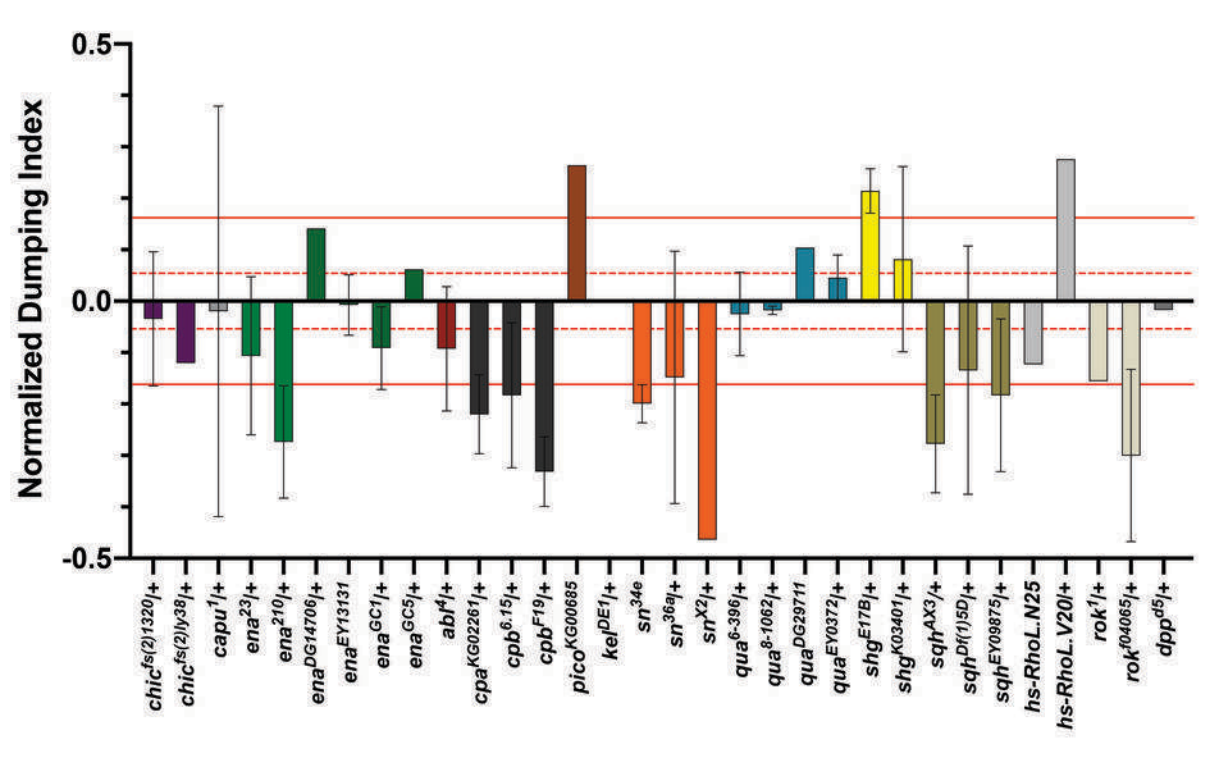
Normalized Dumping Index
0.5
0.0
-0.5
chic^fs(2)1320/+
chic^fs(2)ly38/+
capu^1/+
ena^23/+
ena^210/+
ena^DG14706/+
ena^EY13131
ena^GC1/+
ena^GC5/+
abl^4/+
cpa^KG02261/+
cpb^6.15/+
cpb^F19/+
pico^KG00685
kel^DE1/+
sn^34e
sn^36a/+
sn^X2/+
qua^6-396/+
qua^8-1062/+
qua^DG29711
qua^EY0372/+
shg^E17B/+
shg^K03401/+
sqh^AX3/+
sqh^Df(1)5D/+
sqh^EY09875/+
hs-RhoL.N25
hs-RhoL.V20/+
rok^1/+
rok^k04065/+
dpp^d5/+

A

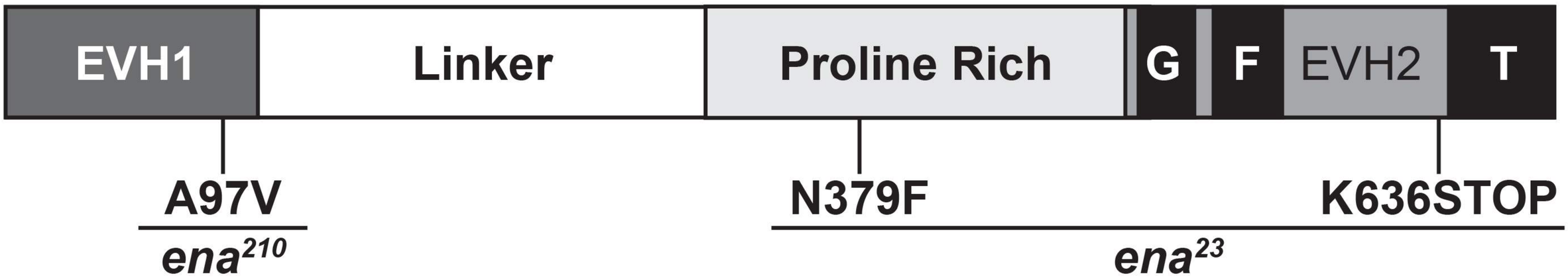
EVH1
Linker
Proline Rich
G
F
EVH2
T
A97V
N379F
K636STOP
ena210
ena23

B

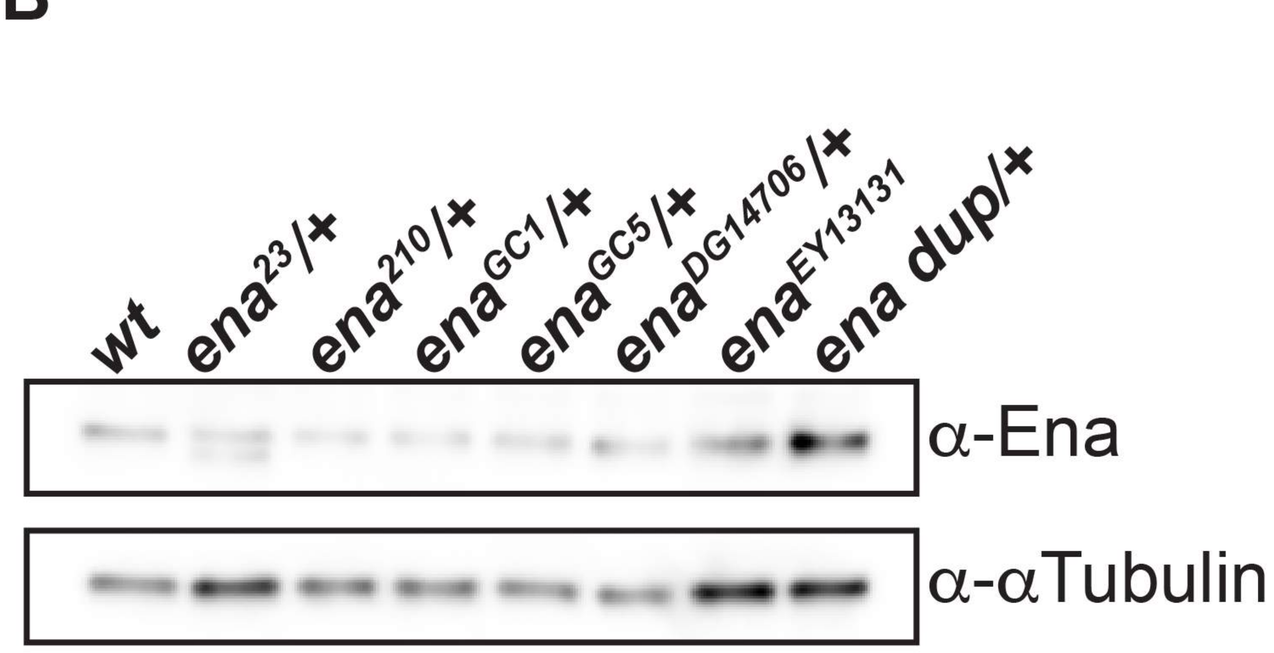
wt
ena23/+
ena210/+
enaGC1/+
enaGC5/+
enaDG14706/+
enaEY13131
ena dup/+
α-Ena
α-αTubulin

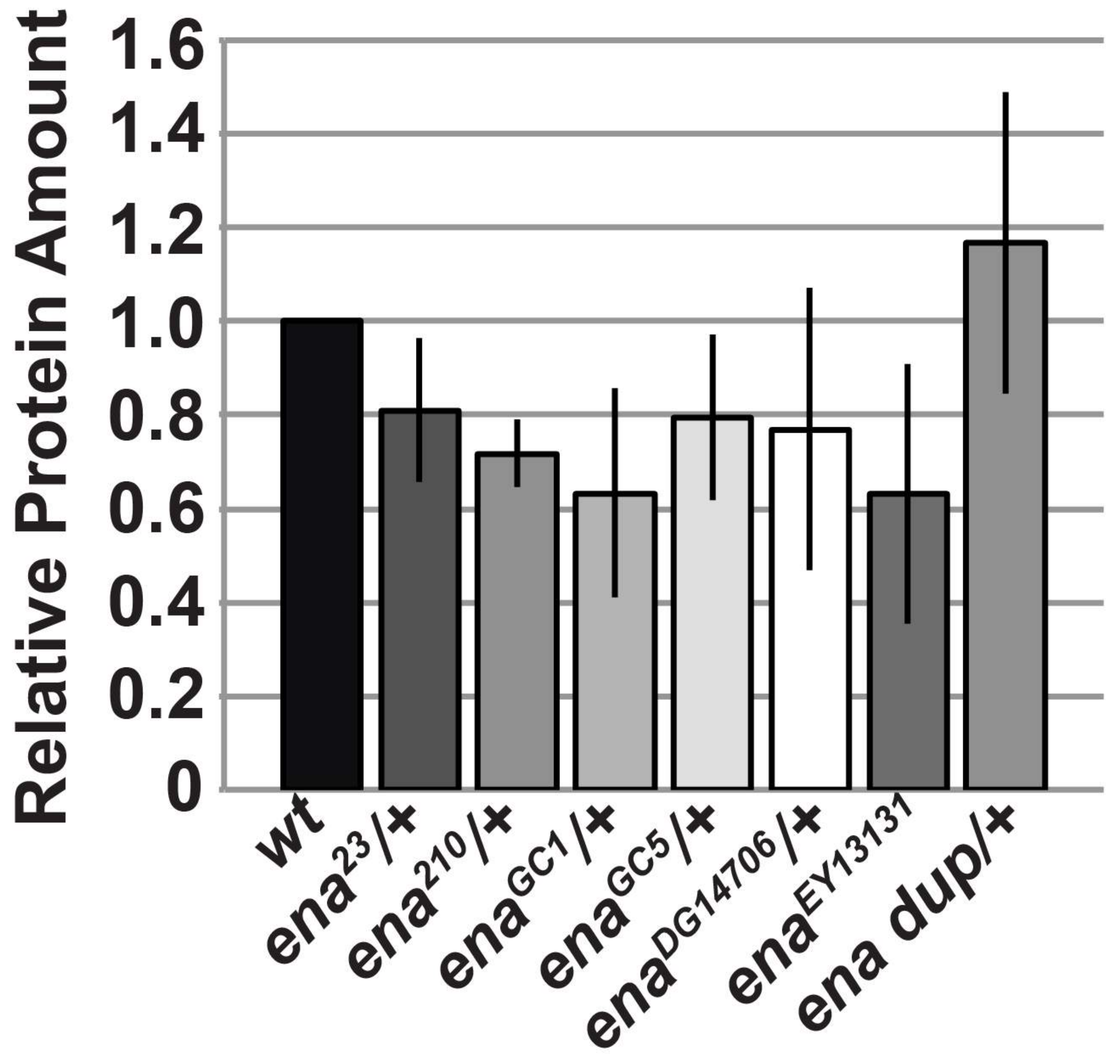
Relative Protein Amount
1.6
1.4
1.2
1.0
0.8
0.6
0.4
0.2
0
wt
ena23/+
ena210/+
enaGC1/+
enaGC5/+
enaDG14706/+
enaEY13131
ena dup/+

C

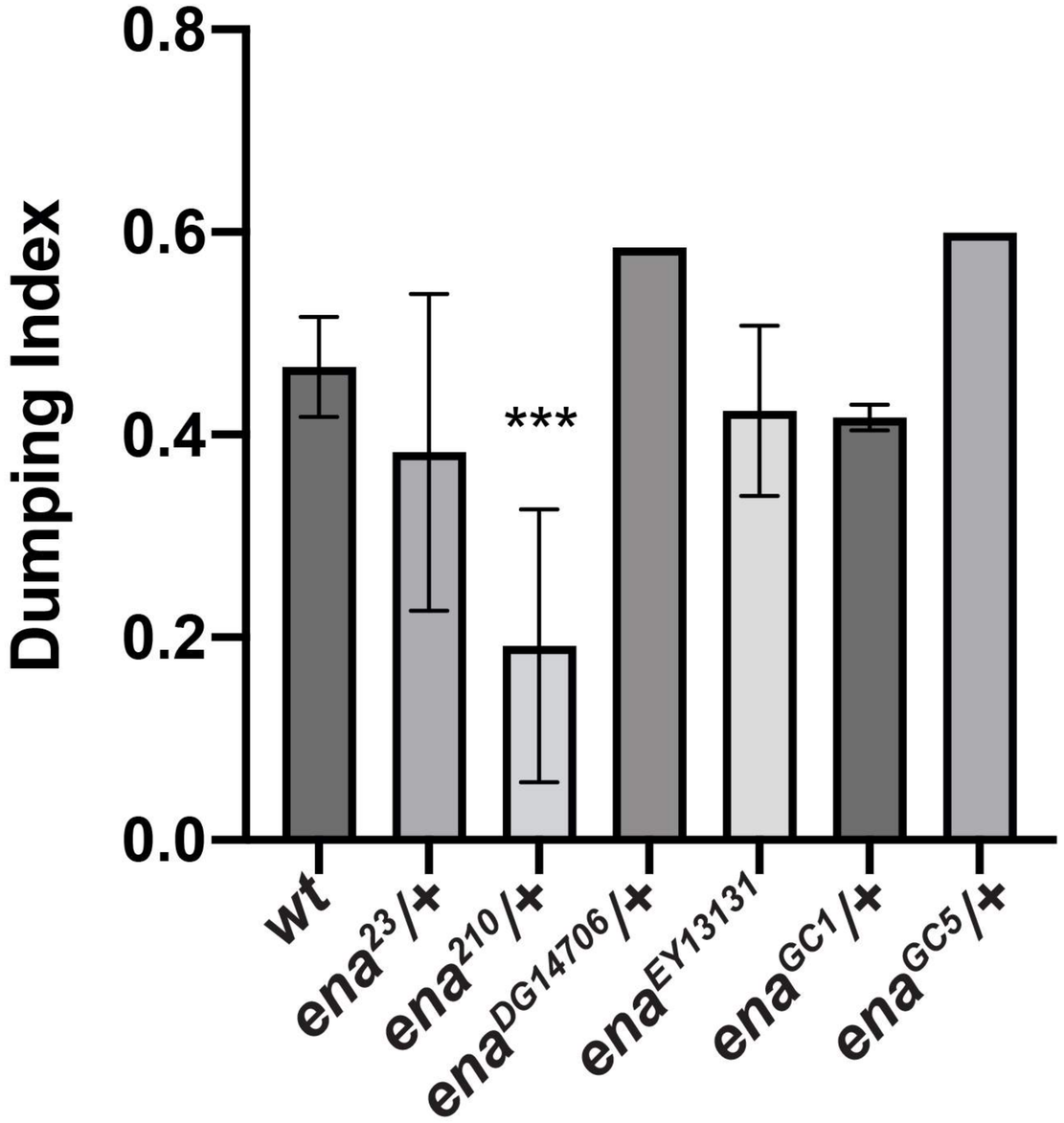
Dumping Index
0.8
0.6
0.4
0.2
0.0
***
wt
ena23/+
ena210/+
enaDG14706/+
enaEY13131
enaGC1/+
enaGC5/+

D

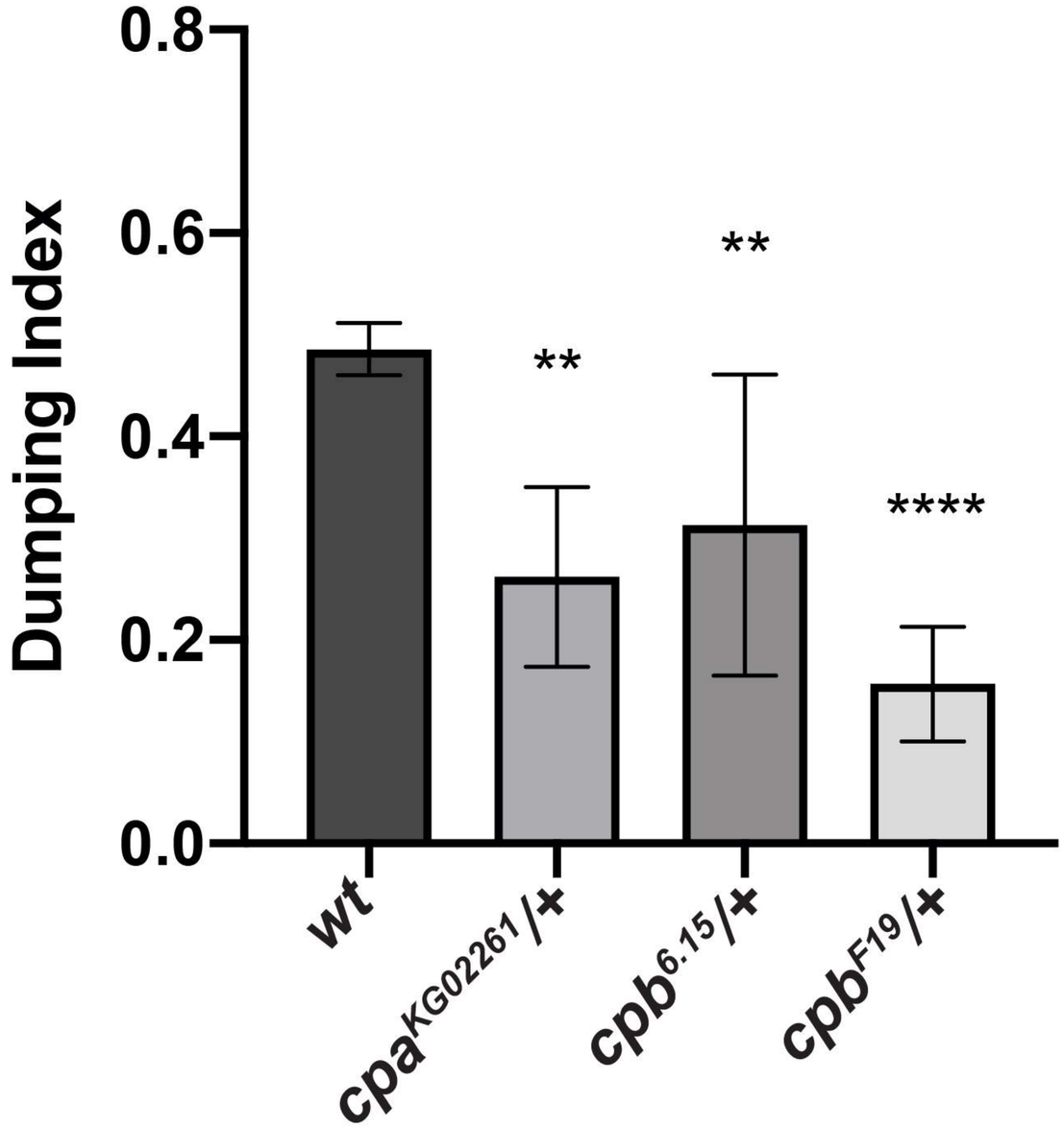
Dumping Index
0.8
0.6
0.4
0.2
0.0
**
**
****
wt
cpaKG02261/+
cpb6.15/+
cpbF19/+

A

Dumping Index

0.8
0.6
0.4
0.2
0

p=0.07

p=0.08

wt

$sqh^{AX3/+}$

$sqh^{Df(1)5D/+}$

$sqh^{EY09875/+}$

B

wt

$pxt^{EY/EY}$

$pxt^{f/f}$

α-Zipper

α-Tubulin

Relative Protein Amount

1.6
1.2
0.8
0.4
0

ns

ns

wt

$pxt^{EY/EY}$

$pxt^{f/f}$

wild-type

pxt -/-

p-MRLC(S19)

C

D

p-MRLC(S19) intensity

C'

D'

Phalloidin

C''

D''

E

p-MRLC membrane intensity

2000
1500
1000
500
0

****

****

wt

$pxt^{EY/EY}$

$pxt^{f/f}$